Check for updates

Journal of Polymer Science

WILEY

JOURNAL OF POLYMER SCIENCE

RESEARCH ARTICLE OPEN ACCESS

Facile, Efficient, and Safe Copper-Free Synthesis of Glycidyl Triazolyl Polymers

Taichi Ikeda[1] | Naoe Hosoda[2,3]

[1]Research Center for Macromolecules and Biomaterials, National Institute for Materials Science, Tsukuba, Japan | [2]Research Center for Materials Nanoarchitectonics, National Institute for Materials Science, Tsukuba, Japan | [3]Tokyo University of Technology, Hachioji, Japan

Correspondence: Taichi Ikeda (ikeda.taichi@nims.go.jp)

Received: 27 February 2025 | **Revised:** 21 April 2025 | **Accepted:** 21 April 2025

Funding: This work was supported by Cabinet Office, Government of Japan, 24126704, Japan Society for the Promotion of Science, 22K05246.

Keywords: azide-alkyne cycloaddition | click chemistry | glycidyl triazolyl polymers | polyethers | post-functionalization of polymers

ABSTRACT

In this study, a new synthetic procxe was proposed to solve the problems in the conventional copper-free glycidyl triazolyl polymer (GTP) synthesis: (1) the explosion risk of the solid glycidyl azide polymer (GAP) and (2) large material loss of the electron-deficient alkyne derivative. In order to demonstrate the superiority of the new synthetic procedure, five kinds of GTPs were synthesized with different types of alkyne derivatives. GAP was synthesized through the reaction between polyepichlorohydrin and sodium azide in *N*,*N*-dimethylformamide. For handling impact- and friction-sensitive solid GAP safely, it was purified through liquid–liquid extraction and stored as a stock solution without isolating it in the solid state. Through the new procedure utilizing a stock solution, the reaction efficiency in GTP synthesis was greatly improved, which resulted in reducing material loss (Feed ratio alkyne/azide: from 4.0 to 1.3) and reaction time (from 72 to 24 h). Thanks to the facile, efficient, and safe synthetic method, enough amounts of GTP samples could be prepared for characterizing not only physicochemical properties (density, molecular weight, glass transition temperature, thermal decomposition temperature, surface free energy) but also mechanical properties (Young's modulus, fracture stress and strain). The synthetic procedure reported herein will accelerate the research and development of functional GTPs with tunable physical properties.

1 | Introduction

The physical properties of polymer materials depend on the polymer design [1–5]. Although the number of polymers that polymer chemists can imagine is nearly infinite, the actual number of polymers that can be synthesized is limited. With the boom of artificial intelligence (AI)-assisted materials design [6–10], it has become important to increase the design capability of polymers. In general, monomers with more complex structures are more difficult to polymerize. The post-functionalization method is an attractive way to expand the design capability of polymer materials because it can skip the obstacles faced in the polymerization process [11–13]. In addition, post-functionalization enables us to prepare a series of polymer materials with the same degrees of polymerization distribution. When the polymer samples are prepared using conventional polymerization methods, the reported physical properties are often different from each other because they have different degrees of polymerization; for instance, the reported values of glass transition temperature (T_g) of poly(*n*-octyl methacrylate) range from −45°C to −20°C [14, 15]. In the case of polymer samples prepared with the post-functionalization method, one can provide high-quality data sets for the machine learning of AI-assisted material design.

Click-chemistry, which won the Nobel Prize in Chemistry 2022, is a powerful tool for post-functionalization [16, 17]. Among the reactions in click-chemistry, the copper-catalyzed azide-alkyne cycloaddition (Cu-AAC) reaction can provide efficient

This is an open access article under the terms of the Creative Commons Attribution License, which permits use, distribution and reproduction in any medium, provided the original work is properly cited.

© 2025 The Author(s). *Journal of Polymer Science* published by Wiley Periodicals LLC.

and functional-group-tolerant (orthogonal) chemistry for post-functionalization [17–22]. Polymer synthesis through post-functionalization with Cu-AAC boomed in the 2000s. However, an accident in a University of Minnesota lab in 2014 reminded chemists of the explosion hazards of azide compounds [23]. Given the above perspectives, the development of safer synthetic procedures is an important issue for the post-functionalization of polymers with AAC.

Glycidyl triazolyl polymer (GTP) is a representative polymer synthesized through post-functionalization with Cu-AAC [24]. Since the first report by H. L. Cohen in 1981 [25], more than 80 types of GTPs, such as ion-conductive GTPs [26–29], GTPs with biocompatible properties [30, 31], and GTPs with self-healing properties [32], have been reported so far. A major advantage of GTP is the ready availability of the starting material polyepichlorohydrin (PECH), which is supplied as Hydrin. As a first step toward GTP, glycidyl azide polymer (GAP) is synthesized through the reaction between PECH and sodium azide (NaN_3) in *N,N*-dimethylformamide (DMF) [25]. In our previous studies, GAP was recovered as a precipitate by adding the reaction solution to water [26–29]. However, storing and handling GAP in the solid state is hazardous because GAP is known as an impact- and friction-sensitive material [33]. In addition, the solubility of solid GAP becomes worse as time goes by because the cross-linking reaction takes place between GAPs [25]. In our experience, GAP stored in the solid state for 2 weeks became less soluble in DMF. These issues concerning the solid GAP have long been an obstacle to accelerating the research and development of GTPs.

As a final step, GTP is synthesized via a Cu-AAC reaction between GAP and an alkyne derivative [26–32]. The use of a copper catalyst requires a time-consuming and stressful work-up procedure for purification. To address this issue, Cu-free synthesis of GTP was previously reported with an AAC reaction between an azide group and an electron-deficient alkyne derivative [25, 34, 35]. However, the results in the previous study discouraged us from exploring new GTPs with Cu-free synthesis because it required much larger amount of alkyne derivative (four equivalent to the azide group) and a long reaction time (72 h) [34].

On the basis of these perspectives, a facile, efficient, and safe synthetic procedure for GTP synthesis was developed in this study. In order to demonstrate the superiority of the new procedure, five kinds of GTPs were synthesized with different types of alkyne derivatives (Figure 1). Octyl (C8), 2-ethyl-hexyl (2Et-C6), *cis*-3-octenyl (*cis*3-C8), 2-(2-methoxyethoxy)ethyl (EG2Me), and benzyl (Bz) groups were selected as the side groups for modulating the physical properties of GTPs. Those side groups were representatives of linear alkyl, branched alkyl, kink alkenyl, flexible ethylene oxide, and aromatic groups. Although polymethacrylate derivatives with the C8, 2Et-C6, EG2Me, and Bz side groups have been reported so far [14, 36–38], there is no report on those with the *cis*3-C8 side group, indicating that the GTP synthesis reported herein can expand the design capability of polymer materials. Thanks to the facile synthetic method, enough amounts of GTP samples could be prepared to characterize not only physicochemical properties (density, molecular weight, glass transition temperature, thermal decomposition temperature, and surface free energy) but also mechanical properties (Young's modulus, fracture stress, and strain).

2 | Results and Discussion

2.1 | Synthesis of Electron-Deficient Alkynes

Figure 2a shows the synthetic route for the electron-deficient alkyne derivatives. In our previous study, electron-deficient alkyne derivatives were synthesized through a transesterification reaction between the alcohol and methyl propiolate in the presence of *p*-toluenesulfonic acid as an acid catalyst [34]. Despite the long reaction time (72 h), the product yield was low (43%). In this study, electron-deficient alkynes were synthesized through an esterification reaction between alcohol and propiolic acid in the presence of cation exchange resin as an acid catalyst. We succeeded in reducing the reaction time (24 h) and improving the product yield. Because the product was obtained almost quantitatively (yield > 90%), the synthesis of alkyne-C8 and alkyne-2Et-C6 required no silica gel chromatography purification. The synthesis of alkyne-EG2Me could also skip chromatography purification because the unreacted materials could be removed in a liquid–liquid partition process (toluene/water). In the cases of alkyne-*cis*3-C8 and alkyne-Bz, side reactions decreased the product yields and required chromatography purification. After the reaction, the cation exchange resin was recovered from the reaction solution by filtration. When the

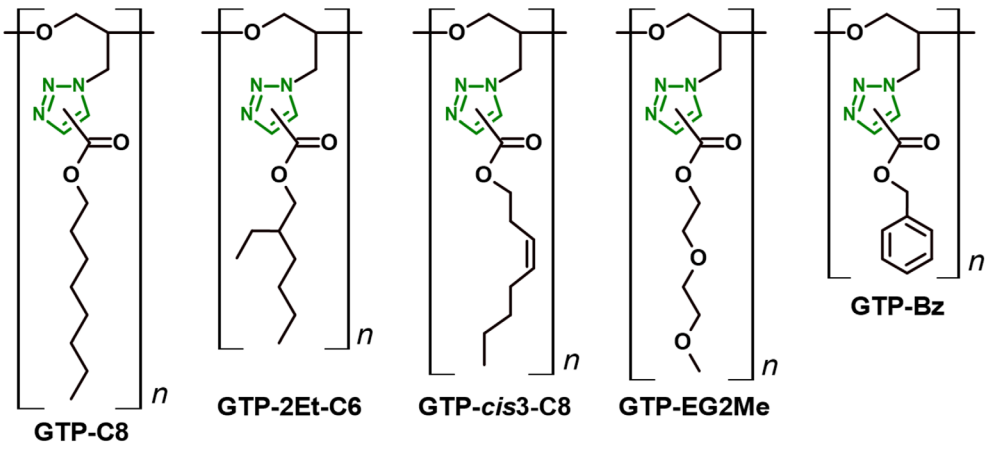

FIGURE 1 | Chemical structures of GTPs.

26424169, 2025, 12, Downloaded from https://onlinelibrary.wiley.com/doi/10.1002/pol.20250233 by National Institute For, Wiley Online Library on [15/06/2025]. See the Terms and Conditions (https://onlinelibrary.wiley.com/terms-and-conditions) on Wiley Online Library for rules of use; OA articles are governed by the applicable Creative Commons License

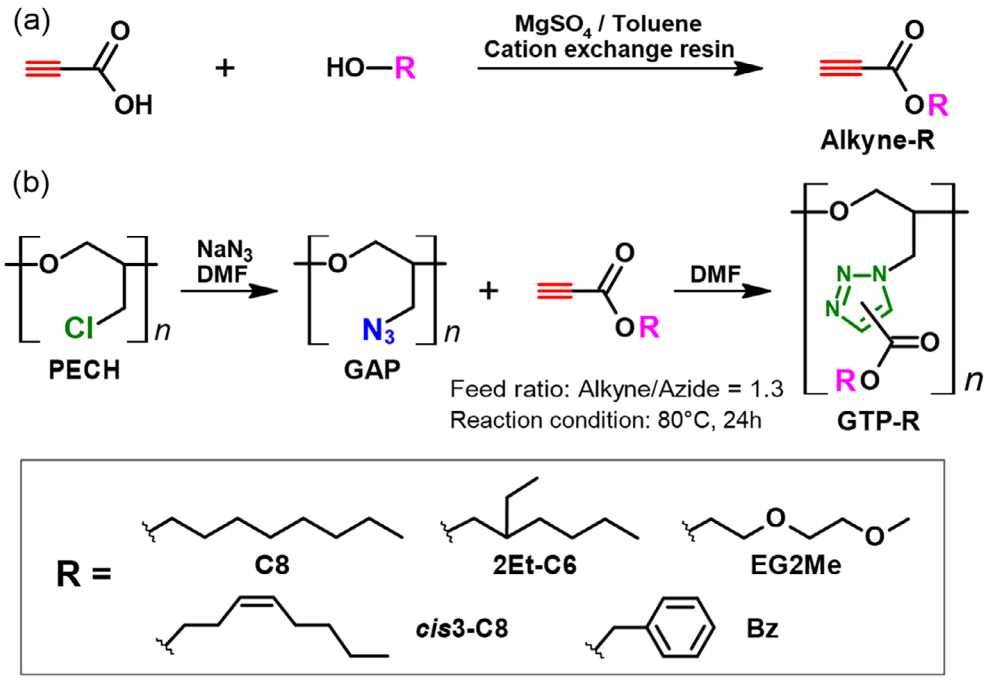

FIGURE 2 | Synthetic route for GTP. (a) Synthesis of electron-deficient alkyne derivatives. (b) Cu-free synthesis of GTP.

reaction was carried out using the recovered cation exchange resin, the product yield decreased to 60%, confirming that the cation exchange resin could not be reused. The reaction temperature (100°C) is close to the upper limit of the suggested operating condition of the resin (5°C–120°C). Thermal degradation is a possible reason for the performance deterioration of the resin as an acid catalyst.

2.2 | Cu-Free Synthesis of GTPs

Figure 2b shows the synthetic route for the GTP derivatives. First, GAP was synthesized from PECH through a reaction with NaN_3. Reportedly, the formation of hydrazoic acid through the reaction between water and NaN_3 was a plausible cause of the explosion at the incident at the University of Minnesota in 2014 [23]. During the reaction, continuous N_2 purge effectively prevented the accumulation of hydrazoic acid in the reaction solution because hydrazoic acid is easily volatile [39]. After the reaction was completed, the solution was cooled to room temperature and diluted with ethyl acetate. Then, distilled water (100 mL) was added to the reaction mixture with stirring to dissolve salts (NaCl and unreacted NaN_3). When the aqueous layer was collected using a separation funnel, its volume increased to ~170 mL, indicating that a large amount of DMF was partitioned to the aqueous layer. To prevent the formation of a highly concentrated GAP solution, dry DMF (30 mL) was added before the evaporation. The solvent ethyl acetate was removed using an evaporator at 40°C under reduced pressure. Complete removal of ethyl acetate was confirmed by ^{1}H NMR of the stock solution (data not shown). The weight of the GAP stock solution was adjusted by adding dry DMF. In order to confirm the amount of GAP in the stock solution, solid GAP was recovered by adding 2.0 g GAP stock solution into distilled water. The weight of the recovered GAP was 0.128 ± 0.001 g (average ± standard error, $n = 3$), indicating 80.0 g stock solution contains ca. 5.1 g GAP.

GTP was synthesized through a reaction between GAP and the electron-deficient alkyne derivatives. The reaction mixture was prepared by adding electron-deficient alkyne derivatives directly to the stock solution of GAP. Compared with our previous study [34], the reaction time was shortened from 72 to 24 h. The feed ratio of alkyne to azide (alkyne/azide) was also improved from 4.0 to 1.3, which is a big advantage in decreasing the material loss of the alkyne derivatives. The key for improving the reaction efficiency was a higher reaction temperature (this study: 80°C; previous study: 60°C). In our previous study, the reaction temperature could not be raised to suppress the discoloration of GTP. In recent years, we empirically realized that salt contamination was one of the causes of discoloration. In the previous study, GAP was recovered as a precipitate by adding GAP solution to water [26–29, 34]. In that case, the salt inside the solid GAP was difficult to remove completely. In order to confirm desalination efficiency, the weight of the recovered salt through the work-up process was measured in 1.0 g scale GAP synthesis (see Supporting Information). In the case of the conventional procedure (precipitation in distilled water), the weight of the recovered salt was 0.82 ± 0.02 g (average ± standard error, $n = 3$). The new work-up procedure reported herein could recover 0.92 ± 0.00 g salts (average ± standard error, $n = 3$), which was close to the theoretical maximum of 0.93 g. The small standard error indicates that the new work-up procedure is reliable for complete removal of salts. The concentration of the solution was also an important factor in improving the reaction efficiency (this study: 1.0 g GAP per 16 mL of DMF; previous study: 1.0 g GAP per 50 mL of DMF). In the previous study, a large amount of solvent was required to dissolve solid GAP. The stock solution method reported herein contributed to improving not only the safety but also the efficiency of the reaction. As mentioned above, the solubility of the solid GAP became worse in 2 weeks because of the cross-linking reaction between GAPs [25]. When the stock solution was stored in a desiccator under dark, no deterioration was detectable in 2 weeks.

26424169, 2025, 12, Downloaded from https://onlinelibrary.wiley.com/doi/10.1002/pol.20250233 by National Institute For, Wiley Online Library on [15/06/2025]. See the Terms and Conditions (https://onlinelibrary.wiley.com/terms-and-conditions) on Wiley Online Library for rules of use; OA articles are governed by the applicable Creative Commons License

The chemical structure of GTP was confirmed using ^{1}H NMR, ^{13}C NMR, and IR spectra. Figure 3 shows the ^{1}H NMR spectrum of GTP-*cis*3-C8. The peaks were assigned with the help of 2D COSY and HMQC spectra (Figures S11 and S12). The integral value of each peak matches the chemical structure (Figure S13). The peaks of the glycidyl protons a and c and the triazole proton d were split because of the stereochemistry of the carbon b. From the integrals of the triazole peaks, the ratio of 1,4-substituted and 1,5-substituted GTPs was calculated to be 9:1. The formation of structural isomer was a drawback of Cu-free synthesis of GTP [34, 35]. It was confirmed that the ratio of 1,4- and 1,5-substituted products was almost independent of the reaction conditions and type of substituents in this study (Table 1). Figure S14 shows the IR spectra of GAP and GTPs. It was confirmed that the azide peak ($\nu = 2100\,cm^{-1}$) disappeared in the spectra of GTPs, indicating quantitative conversion from the azide group to the triazole group. All GTPs exhibited a characteristic strong peak at $1728\,cm^{-1}$ based on C═O stretching.

The densities of PECH, GAP, and GTPs are summarized in Table 1. The density of PECH was comparable to the reported value ($1.41\,g\,cm^{-3}$) in the technical data sheet published by the vendor (Scientific Polymer Products). The density of GAP was also consistent with the literature value [33]. The densities of GTP-C8, GTP-2Et-C6, and GTP-*cis*3-C8 were around $1.15\,g\,cm^{-3}$, which was comparable to that of Nylon 66 ($1.14\,g\,cm^{-3}$) [40]. GTP-EG2Me and GTP-Bz gave higher densities of around $1.30\,g\,cm^{-3}$ because of the introduction of additional oxygen atoms and the aromatic group, respectively. These densities were comparable to that of polyether ether ketone ($1.32\,g\,cm^{-3}$) [41].

Figure 4 shows the molecular weight distributions of PECH, GAP, and GTPs determined using size exclusion chromatography (SEC) with polystyrene standards. The number and weight average molecular weights (M_n and M_w) and polydispersity index (PDI) are summarized in Table 1. The M_n value of PECH was comparable to the reported value in the vendor's technical

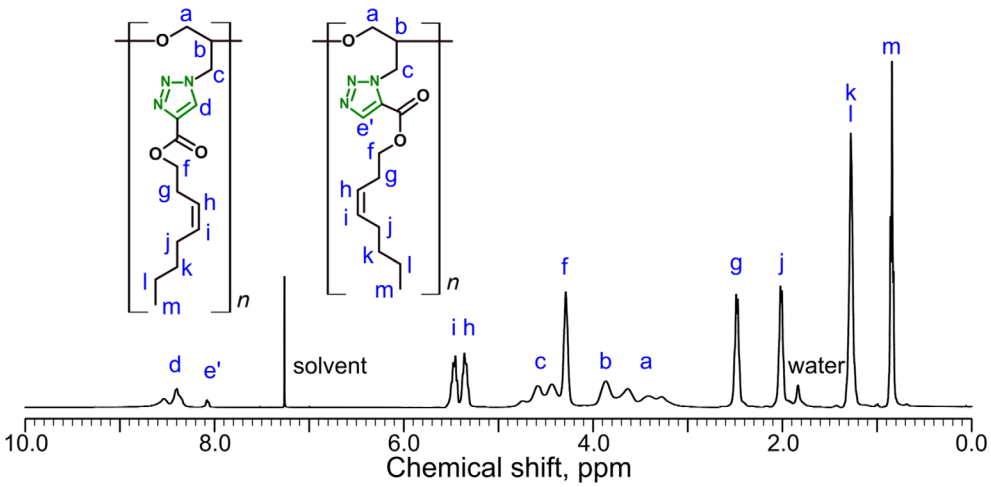

FIGURE 3 | ^{1}H NMR spectrum of GTP-*cis*3-C8. (400 MHz, solvent: $CDCl_3$). Assignments of peaks are also depicted.

TABLE 1 | Density, molecular weights, and thermal properties of PECH, GAP, and GTPs.

Polymers	Ratio of isomers[a]	ρ[b] [g cm^{-3}]	M_n[c] [g mol^{-1}]	M_w[d] [g mol^{-1}]	PDI[e]	T_g[f] [°C]	T_{d5}[g] [°C]
PECH	—	1.40	6.6×10^5	3.7×10^6	5.5	−25	329
GAP	—	1.29	6.0×10^5	2.6×10^6	4.4	−43	219
GTP-EG2Me	9:1	1.32	4.2×10^5	9.7×10^5	2.3	4	273
GTP-*cis*3-C8	9:1	1.16	3.9×10^5	1.0×10^6	2.6	12	299
GTP-2Et-C6	9:1	1.14	3.0×10^5	5.9×10^5	2.0	20	323
GTP-C8	9:1	1.14	3.6×10^5	8.4×10^5	2.4	29	304
GTP-Bz	9:1	1.31	4.4×10^5	9.6×10^5	2.2	63	265

[a]1,4-substituted GTP: 1,5-substituted GTP.
[b]Density.
[c]Number average molecular weight.
[d]Weight average molecular weight.
[e]Polydispersity index.
[f]Glass transition temperature (onset value).
[g]5 wt% loss temperature (onset value).

26424169, 2025, 12, Downloaded from https://onlinelibrary.wiley.com/doi/10.1002/pol.20250233 by National Institute For, Wiley Online Library on [15/06/2025]. See the Terms and Conditions (https://onlinelibrary.wiley.com/terms-and-conditions) on Wiley Online Library for rules of use; OA articles are governed by the applicable Creative Commons License

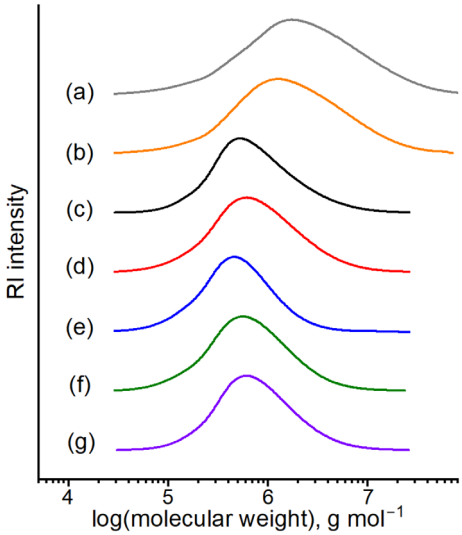

FIGURE 4 | Molecular weight distributions of GTPs. Polystyrene standard. (a) PECH. (b) GAP. (c) GTP-EG2Me. (d) GTP-*cis*3-C8. (e) GTP-2Et-C8. (f) GTP-C8. (g) GTP-Bz.

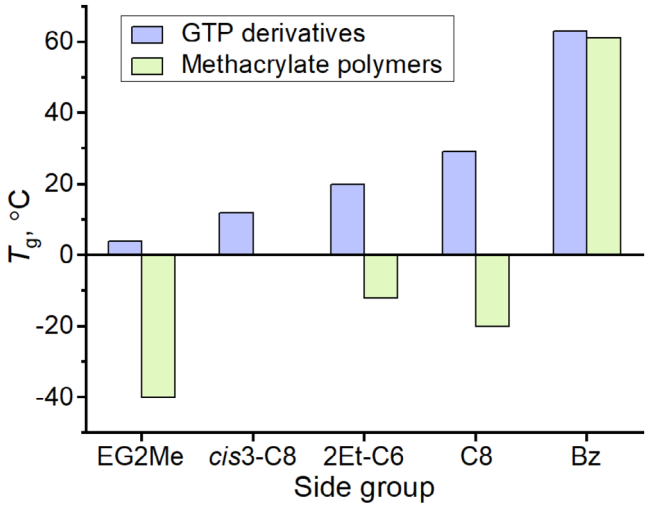

FIGURE 5 | Glass transition temperatures (T_g) of GTP derivatives and methacrylate polymers. The T_g values of methacrylate polymers are applied as representative reference values [14, 36–38]. No data was found for methacrylate polymer with a *cis*3-C8 side group.

data sheet (7.0×10^5 g mol^{-1}, Scientific Polymer Products). The PDI values of PECH and GAP were very large, suggesting that these polymers would aggregate in the solution. The molecular weights and PDI values of GTPs were smaller than those of PECH and GAP. This result also supports the speculation that PECH and GAP would aggregate in the solution. The same results have been reported in our previous studies [26–29, 34, 35]. It was confirmed that the molecular weight distributions were similar for all GTPs. Looking into the detail, GTP-2Et-C6 exhibited the smallest M_n and PDI values among GTPs. The branched side chain is considered to be effective to suppress aggregation.

2.3 | Thermal Properties of GTPs

The thermal properties of PECH, GAP, and GTPs were characterized using differential scanning calorimetry (DSC) and thermogravimetric analysis (TGA). Figure S15 shows the DSC charts of PECH, GAP, and GTPs in the third heating cycle. The T_g values are summarized in Table 1. PECH and GAP were amorphous rubber materials with T_g values of −25°C and −43°C, respectively. As for GAP, an exothermic peak was observed above 170°C due to the azide group decomposition.

When the GTP sample solutions were added dropwise in the poor solvent (methanol or diethyl ether), some GTPs were recovered as white solid materials, indicating crystal domain formations. Figure S16 shows the DSC charts of GTPs in the first heating cycle. GTP-2Et-C8, GTP-C8, and GTP-Bz clearly exhibited the endothermic peaks attributable to the melting of the crystal domains. In the third heating cycle in Figure S15, all DSC charts exhibited only heat capacity change based on the glass transition. After thermal treatment, samples became transparent, indicating that GTPs reported herein are amorphous materials and the crystal domains in GTPs are kinetically trapped metastable states. The T_g values of GTPs are summarized in Figure 5. The T_g values were modulated around room temperature by changing the design of the side group. Compared with the linear alkyl chain (C8), the branched alkyl chain (2Et-C6) and the kink alkenyl chain (*cis*3-C8) decreased the T_g value. The flexible ethylene oxide chain (EG2Me) was the most effective in decreasing the T_g value. Meanwhile, the rigid aromatic ring of the benzyl group (Bz) increased the T_g value. As references, the T_g values of methacrylate polymers are also shown in Figure 5 [14, 36–38]. Except for the Bz side group, the T_g values of GTPs were much higher than those of the methacrylate polymers. This was attributed to much higher molecular weights of GTPs reported herein. The M_n values of the methacrylate polymers with EG2Me, 2Et-C6, and Bz groups were 2.7×10^4, 5.3×10^4, and 1.1×10^5 g mol^{-1}, respectively [36–38].

Figure S17 shows the TGA charts of PECH, GAP, and GTPs. The 5 wt% loss temperatures (T_{d5}) are summarized in Table 1. The T_{d5} value of PECH was above 300°C. As for GAP, a stepwise weight drop was observed in the temperature range from 180°C to 300°C. The weight loss in this step was 0.42, which is consistent with the weight loss of the azide group (molecular weights of azide group/monomer unit = 42.02/99.09 = 0.42). The T_{d5} values of GTPs with the alkyl chains (C8 and 2Et-C6) were above 300°C. The T_{d5} value of GTP-*cis*3-C8 was also comparable to that of GTP-C8. Meanwhile, the ethylene oxide chain made the T_{d5} value worse. GTP-EG2Me lost 2 wt% mass up to 200°C, presumably due to the evaporation of water. It was considered that the ether oxygen atoms of the ethylene oxide chains could catch water molecules. Compared with the methacrylate analogue, which was reported to be extremely hygroscopic [37], GTP-EG2Me exhibited little hygroscopic nature because it could form hydrophobic surfaces, as discussed below. GTP-Bz afforded the worst T_{d5} value (265°C) among GTPs reported in this study. The benzyl ester was susceptible to thermal decomposition, which was also reported for poly(benzyl methacrylate) [42].

2.4 | Mechanical Properties of GTPs

The mechanical properties of PECH and GTPs were characterized by tensile tests. The results are summarized in Table 2.

26424169, 2025, 12, Downloaded from https://onlinelibrary.wiley.com/doi/10.1002/pol.20250233 by National Institute For, Wiley Online Library on [15/06/2025]. See the Terms and Conditions (https://onlinelibrary.wiley.com/terms-and-conditions) on Wiley Online Library for rules of use; OA articles are governed by the applicable Creative Commons License

Figure 6 shows the stress–strain curves of GTPs. As shown in the inset photograph in Figure 6, the specimens of GTPs were transparent because they were amorphous polymers, as discussed above. It was confirmed that the mechanical properties were linked to the glass transition temperature. GTPs with a higher glass transition temperature were harder; consequently, they exhibited smaller fracture strains and larger Young's moduli. In the cases of GTP-Bz and GTP-C8, the specimens fractured before yielding because their T_g values (63°C and 29°C, respectively) were higher than room temperature (16°C–17°C). In the case of GTP-2Et-C6, the specimen was fractured just after yielding because the T_g value (20°C) was near room temperature. In the case of GTP-*cis*3-C8, necking and strain hardening processes were observed because the T_g value (12°C) was below room temperature. The maximum stress was observed at the fracture strain. In the case of GTP-EG2Me, fracturing did not occur up to 700% strain. Because of its much lower T_g value (4°C) than room temperature, GTP-EG2Me was soft and easily deformed by stretching. Even if the stretch rate increased up to 100 mm min^{-1}, fracturing was not observed. As a reference, the mechanical property of PECH was also characterized (Figure S18). Young's modulus of PECH was smaller than that of GTP-EG2Me because of its low T_g value.

TABLE 2 | Mechanical properties of GTPs (average ± standard error, $n = 3$).

Polymers	E [MPa][a]	σ_f [MPa][b]	ε_f [%][c]	T_g [°C][d]
PECH	0.86 ± 0.01	> 0.8[e]	> 700[e]	−25
GTP-EG2Me	2.9 ± 0.4	> 0.8[e]	> 700[e]	4
GTP-*cis*3-C8	100 ± 10	13 ± 1	570 ± 20	12
GTP-2Et-C6	190 ± 10	14 ± 1	13 ± 1	20
GTP-C8	410 ± 40	22 ± 1	9.3 ± 0.9	29
GTP-Bz	870 ± 120	16 ± 1	3.3 ± 0.8	63

[a]Young's modulus.
[b]Fracture stress.
[c]Fracture strain.
[d]Glass transition temperature.
[e]PECH and GTP-EG2Me did not fracture up to 700% strain.

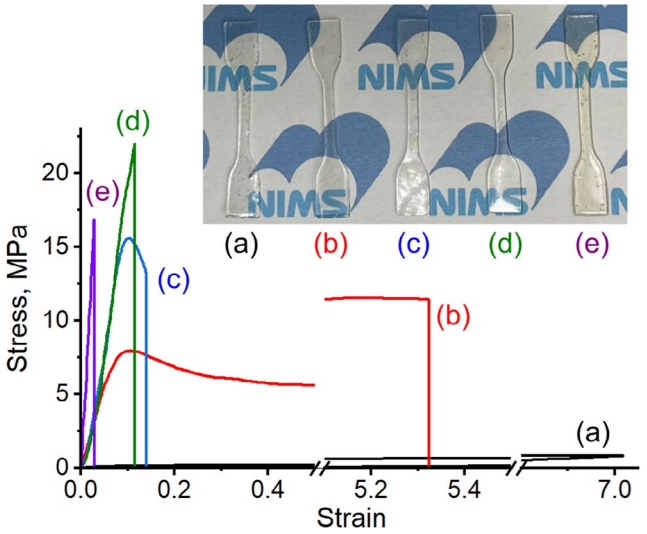

FIGURE 6 | Stress–strain curve of GTPs. Stretch rate: 10 mm min^{-1}. Temperature: Room temperature (16°C–17°C). (a) GTP-EG2Me. (b) GTP-*cis*3-C8. (c) GTP-2Et-C6. (d) GTP-C8. (e) GTP-Bz. Inset photograph: Dumbbell-shaped specimens of GTPs.

2.5 | Surface Free Energy of GTPs

The surface free energies of PECH and GTPs were characterized by contact angle measurements. From the contact angles obtained with water, ethylene glycol, and diiodomethane droplets, dispersive and polar components of the surface energy (γ^d and γ^p, respectively) were calculated [43]. The results are summarized in Table 3 and Figure 7. For all GTPs and PECH, dispersive interaction was the major component of the surface energy. The surface free energy of GTP-EG2Me was comparable to that of GTP-C8 even though GTP-EG2Me had a relatively polar ether oxygen group. It is considered that the surface free energy would be determined by the hydrophobicity of the terminal methyl group. In comparison, GTP-*cis*3-C8 and GTP-2Et-C6 gave higher surface energies. The introduction of a kink (*cis*3-C8) and branched (2Et-C6) points increased the degree of disorder, which might expose a relatively higher energy surface of the glycidyl triazolyl unit. GTP-Bz exhibited the highest surface energy among GTPs reported herein. The polymethacrylate analogs also showed a similar trend (diamond dots in Figure 7)

TABLE 3 | Contact angle and surface free energy of GTPs (average ± standard error, $n = 3$).

Polymers	θ_{water} [°][a]	θ_{EG} [°][b]	θ_{DIM} [°][c]	γ^d [mN m^{-1}][d]	γ^p [mN m^{-1}][e]
PECH	98.0 ± 1.4	68.2 ± 0.2	41.8 ± 3.8	32.2 ± 9.2	0.1 ± 0.7
GTP-EG2Me	93.8 ± 0.2	70.4 ± 0.2	52.5 ± 1.5	19.4 ± 3.6	3.4 ± 1.5
GTP-*cis*3-C8	88.9 ± 0.3	64.9 ± 0.1	55.0 ± 0.2	29.2 ± 4.8	1.2 ± 1.5
GTP-2Et-C6	97.1 ± 0.8	73.7 ± 0.1	58.0 ± 0.6	29.8 ± 6.9	0.0 ± 0.1
GTP-C8	96.2 ± 0.7	77.8 ± 1.2	66.5 ± 1.5	19.7 ± 5.3	2.4 ± 1.8
GTP-Bz	80.4 ± 0.9	51.5 ± 0.1	31.8 ± 0.1	46.1 ± 1.0	0.1 ± 0.1

[a]Contact angle of water.
[b]Contact angle of ethylene glycol.
[c]Contact angle of diiodomethane.
[d]Dispersive component of the surface energy of GTP.
[e]Polar component of the surface energy of GTP. Temperature: Room temperature (22°C–23°C).

26424169, 2025, 12, Downloaded from https://onlinelibrary.wiley.com/doi/10.1002/pol.20250233 by National Institute For, Wiley Online Library on [15/06/2025]. See the Terms and Conditions (https://onlinelibrary.wiley.com/terms-and-conditions) on Wiley Online Library for rules of use; OA articles are governed by the applicable Creative Commons License

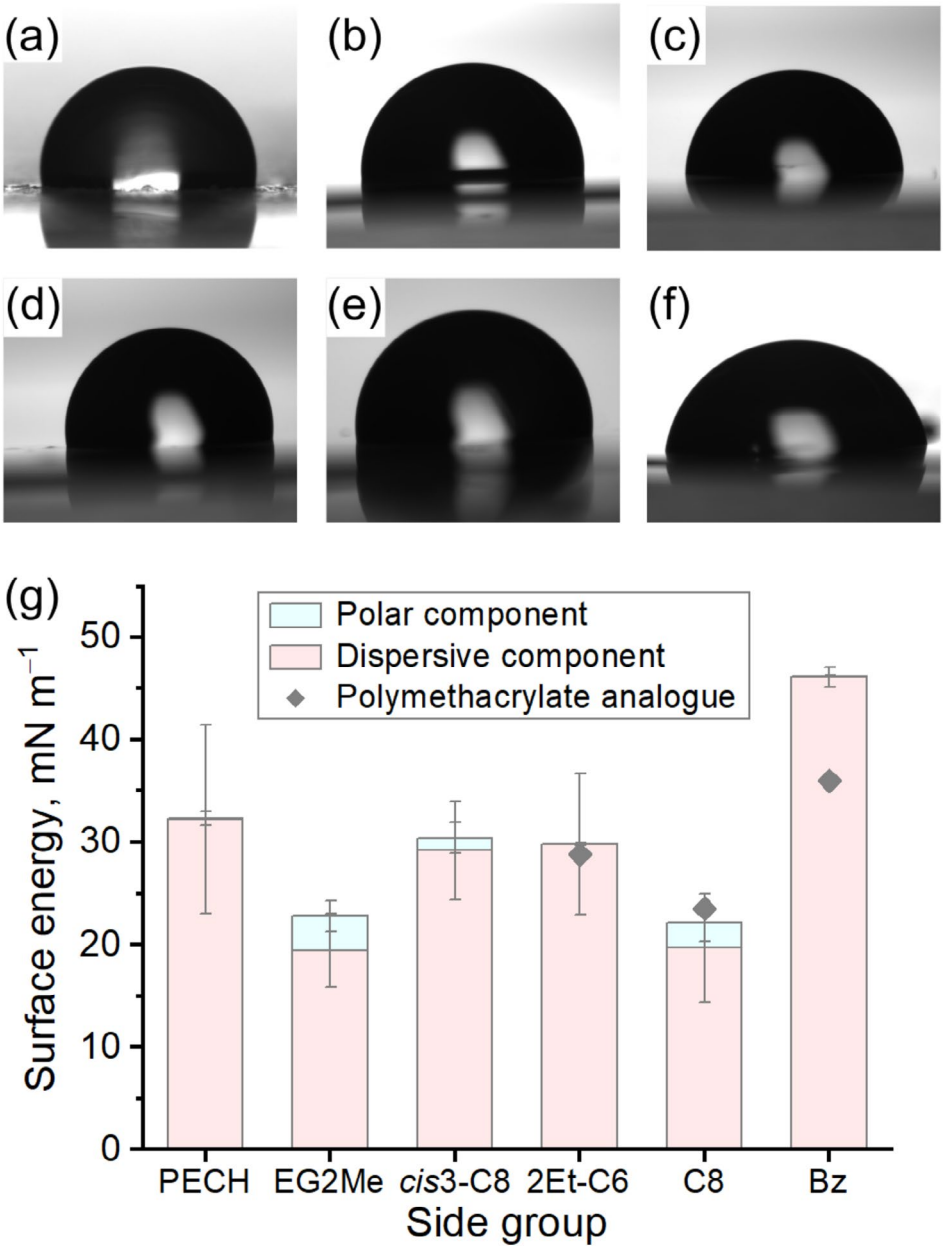

FIGURE 7 | Contact angles of water droplets on (a) PECH, (b) GTP-EG2Me, (c) GTP-*cis*3-C8, (d) GTP-2Et-C6, (e) GTP-C8, and (f) GTP-Bz films. (g) Surface free energy of PECH and GTP films. Diamond dots are plotted as reference data of poly(2-ethyl-hexyl methacrylate), poly(octyl methacrylate), and poly(benzyl methacrylate) [44–46].

[44–46]. It should be noted that GTP-EG2Me was insoluble in water despite poly(2-(2-methoxyethoxy)ethyl methacrylate) being water soluble [37]. These results indicate that GTPs exhibit unique physical properties that cannot be speculated from those of polymethacrylate analogs.

3 | Conclusion

A facile, efficient, and safe synthetic procedure for GTPs was established. Compared to our previous study, the catalyst-free synthesis simplified the work-up process. A new synthetic procedure using a stock solution of GAP reduced the material loss and reaction time. Handling GAP in the solution state improved safety. This method was found to be effective for various types of alkyne derivatives, and the physicochemical and mechanical properties of GTP were successfully modulated. The mechanical properties of GTPs depend on the glass transition temperature; that is, GTPs possessing higher glass transition temperatures exhibited higher Young's moduli and lower elasticities. Thanks to the post-functionalization method, the molecular weight distributions of the synthesized GTPs were comparable. This is a great advantage because the molecular weight dependence of the material properties can be neglected, allowing a rigorous discussion of structure–property relationships. In addition, high efficiency and orthogonal chemistry of AAC must increase the design capability of polymers. The synthetic procedure reported herein will accelerate the research and development of functional GTPs with tunable physical properties.

26424169, 2025, 12, Downloaded from https://onlinelibrary.wiley.com/doi/10.1002/pol.20250233 by National Institute For, Wiley Online Library on [15/06/2025]. See the Terms and Conditions (https://onlinelibrary.wiley.com/terms-and-conditions) on Wiley Online Library for rules of use; OA articles are governed by the applicable Creative Commons License

4 | Experimental Section/Methods

4.1 | Materials

Polyepichlorohydrin (Average molecular weight: 700 kg mol^{-1}) was purchased from Scientific Polymer Products Inc. Propiolic acid, diethylene glycol monomethyl ether, and *cis*-3-octen-1-ol were purchased from Tokyo Chemical Industry. Sodium azide (NaN_3), sodium iodide (NaI), sodium hydroxide (NaOH), anhydrous magnesium sulfate ($MgSO_4$), toluene, dichloromethane, hexane, ethyl acetate, acetone, methanol, 1-octanol, 2-ethyl-1-hexanol, benzyl alcohol, activated carbon, and distilled water were purchased from Nacalai Tesque. Dry DMF was purchased from Kanto Chemical. Cation exchange resin Amberlite HPR2900 H hydrogen form was purchased from Merck. It was washed with distilled water and acetone, then dried under vacuum before use. Polytetrafluoroethylene (PTFE) sheets (thickness: 1 mm) were purchased from AS ONE. Distilled water, ethylene glycol (99.5%) and diiodomethane (97%) for contact angle measurements were purchased from FUJIFILM Wako Pure Chemical.

4.2 | Methods

Column chromatography was done by using Isolera Prime with Sfär Silica HC D flash chromatography cartridges (Biotage Co.). NMR spectra were recorded on a JEOL ECZ 400S (400 MHz and 100 MHz for ^{1}H and ^{13}C nuclei, respectively) with residual solvent as the internal standard. IR spectra were obtained using a Shimadzu IRSpirit-X with a KBr sample pellet. Size exclusion chromatography was carried out at 50°C with 0.01 M Li•NTf_2 in DMF as an eluent on a Shimadzu Nexera XR with a Shim-pack GPC-80MD column. Polystyrene standards (PStQuick A and B, Tosoh Bioscience) were used for molecular weight calibration. DSC was performed on Shimadzu DSC-60 Plus at a heating/cooling rate of 10°C min^{-1} under N_2 flow. TGA was performed with Shimadzu DTG-60 under N_2 flow. Aluminum sample pans were utilized and the heating rate was 10°C min^{-1} up to 550°C under N_2 flow except for the case of GAP. As for GAP, ca. 2.5 mg sample was put in a platinum pan and the heating rate was set as follows: 25°C–180°C: 10°C min^{-1}, 180°C–200°C: 2°C min^{-1}, 200°C–250°C: 1°C min^{-1}, 250°C–280°C: 2°C min^{-1}, 280°C–550°C: 10°C min^{-1}. Polymer density was determined via a sink–float method using NaI aqueous solutions at 20°C. The densities of the solutions were set in the range of 1.10–1.45 g mL^{-1} with a step of 0.01 g mL^{-1}. Films of GTPs were prepared using the hot press machines MP-SCL and MP-SCH (Toyoseiki Co.). GTP samples were heated between two PTFE sheets at 100°C. The pressure was gradually increased up to 5 MPa in 5 min, and the sheets were then cooled to room temperature at 5 MPa. The thickness of the film was controlled with a stainless-steel spacer (Thickness: 0.5 mm). Test specimens for the tensile test were prepared by cutting out GTP films using an ISO 37-4 dumbbell-shaped cutter (Kobunshi Keiki Co.). The tensile test was conducted using a combination of the digital force gage ZTS-50N (Imada Co.) and the vertical motorized test stand MX2-500N (Imada Co.) at room temperature (16°C–17°C). Data were collected using the software Force Logger Next (Ver. 1.05, Imada Co.). The surface free energies of all materials were estimated from contact angle measurements using a drop shape analyzer (DSA25S, Krüss) and the Owens, Wendt, Rabel, and Kaelble method using distilled water, ethylene glycol, and diiodomethane [43]. The films were prepared by drop-casting dichloromethane solutions containing 10 wt% GTP samples on glass plates. The solvent was evaporated at room temperature inside a hood. The films were annealed at 150°C for 1 h and then cooled to room temperature. The laboratory conditions during the contact angle measurements were as follows: a temperature of 22°C–23°C and a relative humidity of 17%–19%.

4.3 | Synthesis

4.3.1 | Synthesis of Alkyne-C8

1-Octanol (13.0 g, 0.10 mol), cation exchange resin (2.5 g), and $MgSO_4$ (5.0 g) were mixed in toluene (50 mL). After 10 min of N_2 bubbling, distilled propiolic acid (9.2 mL, 0.15 mol) was added to the reaction mixture. The reaction solution was heated at 100°C under N_2 atmosphere for 24 h. After cooling to room temperature, the resulting solid materials were removed by filtration. The solid materials on the filter paper were washed using 150 mL of toluene during filtration. The filtrate was washed with distilled water (10 mL) and then with a NaOH aqueous solution (0.40 g/10 mL) using a separation funnel. The organic layer was recovered, dried with $MgSO_4$, filtrated, and concentrated using an evaporator. The colorless liquid product was recovered through distillation (47°C at 2.3 Torr). Yield: 17.1 g (94%). ^{1}H NMR (400 MHz, $CDCl_3$, δ): 0.87 (t, J = 6.8 Hz, 3H), 1.20–1.40 (m, 10H), 1.66 (q, J = 7.2 Hz, 2H), 2.86 (s, 1H), 4.17 (t, J = 6.8 Hz, 2H); ^{13}C NMR (100 MHz, $CDCl_3$, δ): 14.2, 22.7, 25.9, 28.4, 29.2, 31.9, 66.6, 74.5, 74.9, 152.9.

4.3.2 | Synthesis of Alkyne-2Et-C6

2-Ethyl-1-hexanol (13.0 g, 0.10 mol), cation exchange resin (2.5 g), and $MgSO_4$ (5.0 g) were mixed in toluene (50 mL). The reaction condition and work-up process were the same as Alkyne-C8. Distillation condition: 42°C at 2.3 Torr. Yield: 16.4 g (90%). ^{1}H NMR (400 MHz, $CDCl_3$, δ): 0.88 (t, J = 7.6 Hz, 6H), 1.22–1.42 (m, 8H), 1.61 (q, J = 6.0 Hz, 1H), 2.87 (s, 1H), 4.09 (q, J = 3.0 Hz, 2H); ^{13}C NMR (100 MHz, $CDCl_3$, δ): 11.0, 14.1, 23.0, 23.7, 29.0, 30.3, 38.7, 68.8, 74.5, 75.0, 153.1.

4.3.3 | Synthesis of Alkyne-EG2Me

Diethylene glycol monomethyl ether (12.0 g, 0.1 mol), cation exchange resin (2.5 g), $MgSO_4$ (5.0 g) were mixed in toluene (50 mL). The reaction condition and work-up process were the same as Alkyne-C8. Distillation condition: 70°C at 2.3 Torr. Yield: 13.5 g (78%). ^{1}H NMR (400 MHz, $CDCl_3$, δ): 2.94 (s, 1H), 3.32 (s, 3H), 3.49 (t, J = 4.6 Hz, 2H), 3.59 (t, J = 4.6 Hz, 2H), 3.67 (t, J = 4.6 Hz, 2H), 4.28 (t, J = 4.6 Hz, 2H); ^{13}C NMR (100 MHz, $CDCl_3$, δ): 59.0, 65.2, 68.5, 70.5, 71.8, 74.5, 75.4, 152.6.

4.3.4 | Synthesis of Alkyne-cis3-C8

cis-3-Octen-1-ol (12.8 g, 0.10 mol), cation exchange resin (2.5 g), and $MgSO_4$ (5.0 g) were mixed in toluene (50 mL). The reaction

26424169, 2025, 12, Downloaded from https://onlinelibrary.wiley.com/doi/10.1002/pol.20250233 by National Institute For, Wiley Online Library on [15/06/2025]. See the Terms and Conditions (https://onlinelibrary.wiley.com/terms-and-conditions) on Wiley Online Library for rules of use; OA articles are governed by the applicable Creative Commons License

condition and work-up process were the same as Alkyne-C8. Finally, the product was purified by column chromatography (Silica gel, Hexane/Ethyl acetate = 9/1). Distillation condition: 42°C at 2.3 Torr. Yield: 13.5 g (75%). ^{1}H NMR (400 MHz, $CDCl_3$, δ): 0.89 (t, J = 7.2 Hz, 3H), 1.25–1.38 (m, 4H), 2.04 (q, J = 6.8 Hz, 2H), 2.42 (q, J = 7.2 Hz, 2H), 2.87 (s, 1H), 4.18 (t, J = 7.0 Hz, 2H), 5.32 (q, J = 8.4 Hz, 1H), 5.53 (q, J = 8.4 Hz, 1H); ^{13}C NMR (100 MHz, $CDCl_3$, δ): 14.1, 22.4, 26.7, 27.1, 31.8, 65.8, 74.7, 74.9, 123.5, 133.7, 152.8.

4.3.5 | Synthesis of Alkyne-Bz

Benzyl alcohol (10.8 g, 0.10 mol), cation exchange resin (2.5 g), and $MgSO_4$ (5.0 g) were mixed in toluene (50 mL). The reaction condition and work-up process were the same as *Alkyne-cis3-C8*. Distillation condition: 59°C at 2.3 Torr. Yield: 9.5 g (59%). ^{1}H NMR (400 MHz, $CDCl_3$, δ): 2.91 (s, 1H), 5.23 (s, 2H), 7.33–7.43 (m, 5H); ^{13}C NMR (100 MHz, $CDCl_3$, δ): 68.0, 74.6, 75.2, 128.7, 128.8, 128.8, 134.6, 152.6.

4.3.6 | Synthesis of GAP

PECH was cut into small pieces (< 10 mm^3) to facilitate dissolution. PECH (5.0 g, 0.054 mol repeating unit) was suspended in dry DMF (100 mL) in a 500 mL two-neck round-bottom flask with a condenser. After 10 min of N_2 bubbling, NaN_3 (5.0 g, 0.077 mol) was added to the solution at room temperature (note: A plastic spatula was used for weighing NaN_3). The mixture was stirred at 90°C under N_2 flow for 24 h. After cooling to room temperature, the solution was diluted with ethyl acetate (300 mL). Distilled water (100 mL) was added with stirring. The organic layer was recovered with a separation funnel, dried with $MgSO_4$, and filtered. After adding 30 mL of dry DMF, ethyl acetate was completely removed using an evaporator at 40°C under reduced pressure. The weight of the solution was adjusted to 80.0 g by adding dry DMF. This stock solution contains ca. 5.1 g of GAP. The stock solution was stored at room temperature in a desiccator in the dark.

4.3.7 | Synthesis of GTP-C8

After 10 min of N_2 bubbling of the GAP stock solution (16.0 g, 10 mmol repeating unit), Alkyne-C8 (2.4 g, 13 mmol) was added to the solution. The reaction mixture was stirred at 80°C under an N_2 atmosphere for 24 h. After cooling to room temperature, the solution was diluted with acetone (50 mL). The solution was then treated with activated carbon (2.0 g). The activated carbon was removed through filtration (Omnipore hydrophilic PTFE membrane; pore size: 0.45 μm). The solution was concentrated to 20 mL using an evaporator. The product was recovered as a precipitate by adding the solution dropwise to methanol (300 mL) with stirring. The solvent was removed through decantation. The recovered product was dissolved in dichloromethane and concentrated to 20 mL through evaporation. The product was precipitated again in methanol (300 mL). After removing the solvent through decantation, the product was dried under vacuum at 80°C. Yield: 2.6 g (93%). ^{1}H NMR (400 MHz, $CDCl_3$, δ): 0.84 (br, 3H), 1.10–1.50 (br, 10H), 1.72 (br, 2H), 3.10–4.00 (br, 3H), 4.29 (br, 2H), 4.30–4.85 (br, 2H), 8.08 (br, 0.09H), 8.25–8.75 (br, 0.91 H); ^{13}C NMR (100 MHz, $CDCl_3$, δ): 14.2, 22.7, 26.0, 28.6, 28.8, 29.3, 29.4, 31.9, 51.7, 65.6, 67.0–70.5 (br), 77.5–79.0 (overlapping to $CDCl_3$ peak), 129.4, 140.1, 161.0.

4.3.8 | Synthesis of GTP-2Et-C6

After 10 min N_2 bubbling of the GAP stock solution (16.0 g, 10 mmol repeating unit), Alkyne-2Et-C6 (2.4 g, 13 mmol) was added to the solution. The reaction condition and work-up process were the same as GTP-C8. Yield: 2.6 g (92%). ^{1}H NMR (400 MHz, $CDCl_3$, δ): 0.85 (br, 6H), 1.16–1.50 (br, 8H), 1.68 (br, 1H), 3.10–4.00 (br, 3H), 4.21 (br, 2H), 4.32–4.80 (br, 2H), 8.07 (br, 0.09H), 8.32–8.72 (br, 0.91H); ^{13}C NMR (100 MHz, $CDCl_3$, δ): 11.0, 14.1, 23.0, 23.8, 29.0, 30.3, 38.8, 51.7 (br), 67.8, 67.0–70.5 (br), 77.5–78.5 (overlapping to $CDCl_3$), 129.2, 140.1, 161.1.

4.3.9 | Synthesis of GTP-EG2Me

After 10 min N_2 bubbling of the GAP stock solution (16.0 g, 10 mmol repeating unit), Alkyne-EG2Me (2.2 g, 13 mmol) was added to the solution. The reaction condition was the same as GTP-C8. Although the work-up process was almost the same as GTP-C8, diethyl ether was used to precipitate the product instead of methanol. Yield: 2.5 g (92%). ^{1}H NMR (400 MHz, $CDCl_3$, δ): 3.10–4.00 (overlapping, 3H), 3.31 (br, 3H), 3.49 (br, 2H), 3.63 (br, 2H), 3.79 (br, 2H), 4.30–4.80 (overlapping, 2H), 4.46 (br, 2H), 8.13 (br, 0.10 H), 8.30–8.65 (br, 0.90 H); ^{13}C NMR (100 MHz, $CDCl_3$, δ): 51.6 (br), 59.0, 64.3, 67.0–70.5 (br), 69.0, 70.5, 71.9, 77.5–78.5 (overlapping to $CDCl_3$), 129.7, 139.6, 160.8.

4.3.10 | Synthesis of GTP-cis3-C8

After 10 min N_2 bubbling of the GAP stock solution (16.0 g, 10 mmol repeating unit), Alkyne-*cis*3-C8 (2.4 g, 13 mmol) was added to the solution. The reaction condition and work-up process were the same as GTP-C8. Yield: 2.6 g (93%). ^{1}H NMR (400 MHz, $CDCl_3$, δ): 0.84 (br, 3H), 1.28 (br, 4H), 2.01 (br, 2H), 2.48 (br, 2H), 3.10–4.00 (br, 3H), 4.29 (br, 2H), 4.30–4.80 (br, 2H), 5.36 (br, 1H), 5.46 (br, 1H), 8.05 (br, 0.09 H), 8.30–8.75 (br, 0.91 H); ^{13}C NMR (100 MHz, $CDCl_3$, δ): 14.1, 22.4, 27.0, 27.1, 31.8, 51.6 (br), 64.8, 67.0–70.5 (br), 77.5–78.5 (overlapping to $CDCl_3$), 123.8, 129.4, 133.4, 140.1, 160.9.

4.3.11 | Synthesis of GTP-Bz

After 10 min N_2 bubbling of the GAP stock solution (16.0 g, 10 mmol repeating unit), Alkyne-Bz (2.2 g, 14 mmol) was added to the solution. The reaction condition was the same as GTP-C8. Although the work-up process was almost the same as GTP-C8, DMF was used to dilute the reaction solution instead of acetone. Yield: 2.4 g (93%). ^{1}H NMR (400 MHz, $CDCl_3$, δ): 3.00–3.90 (br, 3H), 4.10–4.80 (br, 2H), 5.27 (br, 2H), 7.15–7.40 (br, 5H), 8.05 (br, 0.09H), 8.20–8.60 (br, 0.91H); ^{13}C NMR (100 MHz, $CDCl_3$, δ): 51.4 (br), 66.9, 67.0–70.5 (br), 77.5–78.5 (overlapping to $CDCl_3$), 128.5, 128.7, 128.9, 129.4, 129.7, 135.5, 139.7.

26424169, 2025, 12, Downloaded from https://onlinelibrary.wiley.com/doi/10.1002/pol.20250233 by National Institute For, Wiley Online Library on [15/06/2025]. See the Terms and Conditions (https://onlinelibrary.wiley.com/terms-and-conditions) on Wiley Online Library for rules of use; OA articles are governed by the applicable Creative Commons License

Acknowledgments

This work was supported by Cross-ministerial Strategic Innovation Promotion Program (SIP), Challenge, Strategy, and Research & Development Plan for Social Implementation, 24126704; and Grant-in-Aids for Scientific Research C, 22K05246 (JSPS).

References

1. D. K. Schneiderman and M. A. Hillmyer, "Aliphatic Polyester Block Polymer Design," *Macromolecules* 49 (2016): 2419–2428.

2. H. Takahashi, I. Sovadinova, K. Yasuhara, S. Vemparala, G. A. Caputo, and K. Kuroda, "Biomimetic Antimicrobial Polymers—Design, Characterization, Antimicrobial, and Novel Applications," *Wiley Interdisciplinary Reviews. Nanomedicine and Nanobiotechnology* 15 (2023): e1866.

3. I. Hamerton, B. J. Howlin, and V. Larwood, "Development of Quantitative Structure Property Relationships for Poly(Arylene Ether)s," *Journal of Molecular Graphics* 13 (1995): 14–17.

4. T. Qu, G. Nan, Y. Ouyang, et al., "Structure–Property Relationship, Glass Transition, and Crystallization Behaviors of Conjugated Polymers," *Polymers* 15 (2023): 4268.

5. P. M. Hergenrother, "The Use, Design, Synthesis, and Properties of High Performance/High Temperature Polymers: An Overview," *High Performance Polymers* 15, no. 1 (2003): 3.

6. V. Liao, T. Myers, and A. Jayaraman, "A Computational Method for Rapid Analysis Polymer Structure and Inverse Design Strategy (RAPSIDY)," *Soft Matter* 20 (2024): 8246–8259.

7. Y. Zhao, R. J. Mulder, S. Houshyar, and T. C. Le, "A Review on the Application of Molecular Descriptors and Machine Learning in Polymer Design," *Polymer Chemistry* 14 (2023): 3325–3346.

8. Y. Amamoto, "Data-Driven Approaches for Structure-Property Relationships in Polymer Science for Prediction and Understanding," *Polymer Journal* 54 (2022): 957–967.

9. K. Ishikiriyama, "Polymer Informatics Based on the Quantitative Structure-Property Relationship Using a Machine-Learning Framework for the Physical Properties of Polymers in the ATHAS Data Bank," *Thermochimica Acta* 708 (2022): 179135.

10. F. Cravero, M. F. Díaz, and I. Ponzoni, "Polymer Informatics for QSPR Prediction of Tensile Mechanical Properties. Case Study: Strength at Break," *Journal of Chemical Physics* 156 (2022): 204903.

11. K. A. Günay, P. Theato, and H.-A. Klok, "Standing on the Shoulders of Hermann Staudinger: Post-Polymerization Modification From Past to Present," *Journal of Polymer Science, Part A: Polymer Chemistry* 51 (2013): 1.

12. X. Chen and T. Michinobu, "Postpolymerization Modification: A Powerful Tool for the Synthesis and Function Tuning of Stimuli-Responsive Polymers," *Macromolecular Chemistry and Physics* 223 (2022): 2100370.

13. Y. Zhao, D. Li, and X. Jiang, "Chemical Upcycling of Polyolefins Through C–H Functionalization," *European Journal of Organic Chemistry* 26 (2023): e202300664.

14. S. S. Rogers and L. Mandelkern, "Glass Transitions of the Poly-(n-Alkyl Methacrylates)," *Journal of Physical Chemistry* 61, no. 7 (1957): 985.

15. H. A. Schneider, "Polymer Class Specificity of the Glass Temperature," *Polymer* 46 (2005): 2230–2237.

16. H. C. Kolb, M. G. Finn, and K. B. Sharpless, "Click Chemistry: Diverse Chemical Function From a Few Good Reactions," *Angewandte Chemie International Edition* 40 (2001): 2004.

17. M. Meldal, "Polymer Clicking by CuAAC Reactions," *Macromolecular Rapid Communications* 29 (2008): 1016–1051.

18. V. V. Rostovtsev, L. G. Green, V. V. Fokin, and K. B. Sharpless, "A Stepwise Huisgen Cycloaddition Process: Copper(I)-Catalyzed Regioselective Ligation of Azides and Terminal Alkynes," *Angewandte Chemie, International Edition* 41 (2002): 2596–2599.

19. C. W. Tornøe, C. Christensen, and M. Meldal, "Peptidotriazoles on Solid Phase: [1,2,3]-Triazoles by Regiospecific Copper(I)-Catalyzed 1,3-Dipolar Cycloadditions of Terminal Alkynes to Azides," *Journal of Organic Chemistry* 67 (2002): 3057–3064.

20. W. H. Binder and R. Sachsenhofer, "Click Chemistry in Polymer and Material Science: An Update," *Macromolecular Rapid Communications* 29 (2008): 952–981.

21. E. Haldón, M. C. Nicasio, and P. J. Pérez, "Copper-Catalysed Azide–Alkyne Cycloadditions (CuAAC): An Update," *Organic & Biomolecular Chemistry* 13 (2015): 9528–9550.

22. P. L. Golas and K. Matyjaszewski, "Marrying Click Chemistry With Polymerization: Expanding the Scope of Polymeric Materials," *Chemical Society Reviews* 39 (2010): 1338–1354.

23. T. A. Taton and W. E. Partlo, "Chemical Safety: Explosion Hazard in Synthesis of Azidotrimethylsilane," *Chemical & Engineering News* 92, no. 43 (2014): 2.

24. T. Ikeda, "Glycidyl Triazolyl Polymers: Poly (Ethylene Glycol) Derivatives Functionalized by Azide–Alkyne Cycloaddition Reaction," *Macromolecular Rapid Communications* 39 (2018): 1700825.

25. H. L. Cohen, "The Preparation and Reactions of Polymeric Azides. II. The Preparation and Reactions of Various Polymeric Azides," *Journal of Polymer Science, Part A: Polymer Chemistry* 19 (1981): 3269.

26. T. Ikeda, "Anionic Glycidyl Triazolyl Polymers: Oppositely Charged Analogs of Imidazolium-Based Cationic Glycidyl Triazolyl Polymers," *Macromolecules* 56 (2023): 9229–9236.

27. T. Ikeda, "Poly(Ionic Liquid)s With Branched Side Chains: Polymer Design for Breaking the Conventional Record of Ionic Conductivity," *Polymer Chemistry* 12 (2021): 711–718.

28. M. M. Obadia, A. Jourdain, A. Serghei, T. Ikeda, and E. Drockenmuller, "Cationic and Dicationic 1,2,3-Triazolium-Based Poly(Ethylene Glycol Ionic Liquid)s," *Polymer Chemistry* 8 (2017): 910–917.

29. T. Ikeda, S. Moriyama, and J. Kim, "Imidazolium-Based Poly(Ionic Liquid)s With Poly(Ethylene Oxide) Main Chains: Effects of Spacer and Tail Structures on Ionic Conductivity," *Journal of Polymer Science, Part A: Polymer Chemistry* 54 (2016): 2896–2906.

30. C. Kim, K. Kwon, J. Lee, H. Kim, K.-H. Chae, and M. Ree, "Well-Defined Biomimicking Brush-Polymer Self-Assemblies Revealing Cholesterol-And Phosphorylcholine-Enriched Surface," *Macromolecules* 50 (2017): 6489.

31. J. Lee, J. C. Kim, H. Lee, S. Song, H. Kim, and M. Ree, "Self-Assembling Brush Polymers Bearing Multisaccharides," *Macromolecular Rapid Communications* 38 (2017): 1700013.

32. D. Liu, D. Wang, M. Wang, et al., "Supramolecular Organogel Based on Crown Ether and Secondary Ammoniumion Functionalized Glycidyl Triazole Polymers," *Macromolecules* 46 (2013): 4617.

33. T. Jarosz, A. Stolarczyk, A. Wawrzkiewicz-Jalowiecka, K. Pawlus, and K. Miszczyszyn, "Glycidyl Azide Polymer and Its Derivatives-Versatile Binders for Explosives and Pyrotechnics: Tutorial Review of Recent Progress," *Molecules* 24 (2019): 4475.

34. T. Ikeda, "Copper-Free Synthesis of Glycidyl Triazolyl Polymers," *Macromolecular Chemistry and Physics* 219 (2018): 1800147.

35. T. Ikeda, "Copper-Free Synthesis of Cationic Glycidyl Triazolyl Polymers," *Macromolecular Rapid Communications* 45 (2024): 2400416.

26424169, 2025, 12, Downloaded from https://onlinelibrary.wiley.com/doi/10.1002/pol.20250233 by National Institute For, Wiley Online Library on [15/06/2025]. See the Terms and Conditions (https://onlinelibrary.wiley.com/terms-and-conditions) on Wiley Online Library for rules of use; OA articles are governed by the applicable Creative Commons License

36. C. L. Elkins, T. Park, M. G. Mckee, and T. E. Long, "Synthesis and Characterization of Poly(2-Ethylhexyl Methacrylate) Copolymers Containing Pendant, Self-Complementary Multiple-Hydrogen-Bonding Sites," *Journal of Polymer Science, Part A: Polymer Chemistry* 43 (2005): 4618.

37. S. Han, M. Hagiwara, and T. Ishizone, "Synthesis of Thermally Sensitive Water-Soluble Polymethacrylates by Living Anionic Polymerizations of Oligo(Ethylene Glycol) Methyl Ether Methacrylates," *Macromolecules* 36 (2003): 8312–8319.

38. K. Koike, Q. Du, S. Nishino, and Y. Koike, "Light Scattering of Ideal Random Copolymers in Bulk," *Polymer* 55 (2014): 878–885.

39. D. S. Treitler and S. Leung, "How Dangerous Is Too Dangerous? A Perspective on Azide Chemistry," *Journal of Organic Chemistry* 87 (2022): 11293–11295.

40. Z. Chen, X. Liu, R. Lü, and T. Li, "Friction and Wear Mechanisms of PA66/PPS Blend Reinforced With Carbon Fiber," *Journal of Applied Polymer Science* 105 (2007): 602–608.

41. C. R. C. Lima, M. A. R. Mojena, C. A. D. Rovere, N. F. C. de Souza, and H. D. C. Fals, "Slurry Erosion and Corrosion Behavior of Some Engineering Polymers Applied by Low-Pressure Flame Spray," *Journal of Materials Engineering and Performance* 25 (2016): 4911–4918.

42. K. Demirelli, M. Coskun, and E. Kaya, "Polymers Based on Benzyl Methacrylate: Synthesis via Atom Transfer Radical Polymerization, Characterization, and Thermal Stabilities," *Journal of Polymer Science, Part A: Polymer Chemistry* 42 (2004): 5964.

43. D. K. Owens and R. C. Wendt, "Estimation of the Surface Free Energy of Polymers," *Journal of Applied Polymer Science* 13 (1969): 1741–1747.

44. S. Wu, "Organic Coatings and Plastics Chemistry," 1971, 31, 27.

45. K. Kamagata and M. Toyama, "Effect of the Length of Branches on the Critical Surface Tension of Poly(n-Alkyl Methacrylates) and Copolymers of Stearyl Methacrylate With Methacrylonitrile," *Journal of Applied Polymer Science* 18 (1974): 167–178.

46. M. Toyama, A. Watanabe, and T. Ito, "Surface Wettability of Alkyl Methacrylate Polymers and Copolymers," *Journal of Colloid and Interface Science* 47 (1974): 802–803.

Supporting Information

Additional supporting information can be found online in the Supporting Information section.

26424169, 2025, 12, Downloaded from https://onlinelibrary.wiley.com/doi/10.1002/pol.20250233 by National Institute For, Wiley Online Library on [15/06/2025]. See the Terms and Conditions (https://onlinelibrary.wiley.com/terms-and-conditions) on Wiley Online Library for rules of use; OA articles are governed by the applicable Creative Commons License